Tracer-based high-speed laser-induced fluorescence measurements of temperature and fuel concentration fields in a rapid compression expansion machine

Ulrich Retzer[1], Hannah Ulrich[1,2], Stefan Will[1], Lars Zigan[1,2*]
1: Lehrstuhl für Technische Thermodynamik (LTT) and Erlangen Graduate School in Advanced Optical Technologies (SAOT), Friedrich-Alexander-Universität Erlangen-Nürnberg (FAU), Erlangen, Germany
2: Present address: Institut für Thermodynamik, Professur für Energiewandlung, Fakultät für Luft- und Raumfahrttechnik, Universität der Bundeswehr München, Neubiberg, Germany
* correspondent author: lars.zigan@unibw.de

Keywords: Tracer LIF, burst-mode laser, 2-color LIF, heat transfer

ABSTRACT

Tracer planar laser-induced fluorescence (PLIF) using 1-methylnaphthalene (1-MN) is applied to study temperature and fuel courses during compression in a rapid compression expansion machine (RCEM). A burst mode Nd:YAG-laser at 266 nm is utilized for excitation of tracer fluorescence at a repetition rate of 7.5 kHz. A high-speed intensified CMOS camera equipped with an image doubler is applied for 2-color LIF (2c-LIF). The measurements were conducted in nitrogen atmosphere for which a calibration curve is presented that was generated in a flow cell. The temperature and fuel concentration fields are very homogeneous at early points in time during compression, however, inhomogeneities in terms of millimeter-sized hot and cold gas regions can be found especially near top dead center (TDC). These inhomogeneities were also visible in the fuel partial density field and are due to the distinct heat transfer between the hot gas and the cool walls, and probably also because of roll-up vortices induced by the piston movement. Especially at TDC the minimal gas temperature is about 300 K lower than the peak temperature near the cylinder head. These temperature differences are much larger than in piston engines and in other RCEMs reported in the literature at comparable conditions. This is because of the special design of the present layout of the machine. A relatively large difference to the adiabatic temperature can be overserved particularly at TDC. About 70 K lower temperatures were measured, which can be explained by these temperature inhomogeneities in the cylinder.

1. Introduction

The temperature and fuel dispersion during the mixture formation in internal combustion (IC) engines, industrial burners or gas turbines determine the efficiency of combustion and pollutant emissions. For resolving the local and temporal temperature and species fields, a non-invasive, fast and multidimensional measurement technique is required. Planar laser-induced fluorescence (PLIF) using special tracers is one of the most widely used measurement techniques for investigating the mixture formation (Schulz and Sick 2005).

Toluene is a well-characterized tracer allowing for temperature determination via one color (1c) and two color (2c) detection (Peterson et al. 2015). A simultaneous measurement of temperature and concentration using 2c-LIF is advantageous over 1c-LIF techniques for which certain assumptions are necessary that may introduce further uncertainties (Peterson et al., 2014). For 2c-LIF, the spectral broadening and shift of the fluorescence emission is exploited by building a temperature-dependent ratio over two spectral channels (see also section 2). However, the application of toluene PLIF is hampered at temperatures above 700 K as its fluorescence intensity is reduced strongly with temperature. Anisole is another potential tracer for thermometry based on 2c-LIF, which was applied for mixing studies in IC engines (Tran et al. 2014).

1-methylnaphthalene (1-MN) is a promising tracer for fuel components with high boiling point and shows a large fluorescence signal intensity especially in nitrogen atmosphere. In a previous work of the authors, 1-MN fluorescence has been calibrated in a wide range of pressure, temperature and gas composition (Retzer et al. 2019). This allows for simultaneous determination of fuel concentration (or equivalence ratio) and temperature in an oxygen-containing environment. However, so far all LIF studies based on 1-MN were performed at low repetition rate and at constant pressure conditions.

In general, only few high speed LIF techniques exist for analysis of cyclic occurring phenomena in turbulent reactive flows. One main reason is that existing high-speed lasers are limited in their fluence for excitation of the fluorescence. Burst-mode lasers enable higher pulse energies for such mixing and combustion studies especially in oxygen-containing atmosphere to counteract low signals due to oxygen quenching. High speed diagnostics are necessary as rapid compression and expansion machines (RCEM) cannot be run continuously and only single compressions/expansions are possible. Likewise, optically accessible IC engines require a fast diagnostic technique since they show a thermal drift with operation time or cannot be run for longer times (than usually a few minutes).

This work presents calibration measurements in a flow cell as well as in a RCEM at high pressure and temperature conditions. The LIF measurements in the RCEM are conducted at 7.5 kHz repetition rate using 1-MN PLIF. Afterwards, the PLIF-technique is applied to investigate the fuel and temperature fields under diesel engine conditions close to the wall of the cylinder head. Temperature and fuel partial density are determined simultaneously during the compression and expansion stroke.

2. Measurement principle

The fluorescence signal S_f of a tracer molecule is described by:

$$S_{\mathrm{fl}} \sim \eta \cdot E \cdot n_{\mathrm{tracer}} \cdot \sigma_{\mathrm{abs}}(\lambda_{\mathrm{ex}}, T) \cdot \Phi_{\mathrm{fl}}(\lambda_{\mathrm{ex}}, T, p, \chi_{\mathrm{i}}). \quad (1)$$

The included quantities are:
η: efficiency of the detection system
E: laser fluence
n_{tracer}: number density of tracer molecules
σ_{abs}: absorption cross-section of the tracer molecule
Φ_{fl}: fluorescence quantum yield.

Equation 1 is utilized for the 1-color detection scheme, for which a single LIF image is recorded. There, each pixel contains a spectrally integrated fluorescence signal from a certain volume. A temperature determination is only possible if the image is corrected. This includes correction of laser energy and profile, absorption cross section, tracer number density and optical efficiencies. In principle, a temperature measurement with 1c-LIF just works out for homogeneous conditions. In the present publication, temperature determination is based on 2c detection. Here, the temperature dependent signal ratio of two spectral channels (λ_1 and λ_2) is exploited in case of a variation of the LIF emission spectrum with temperature. This is true for the tracer 1-MN and examples of the temperature dependent shift and broadening of the fluorescence spectra are provided in Figure 1. There, the emission spectra are shown for different ambient gases, namely nitrogen and Biogon C20.

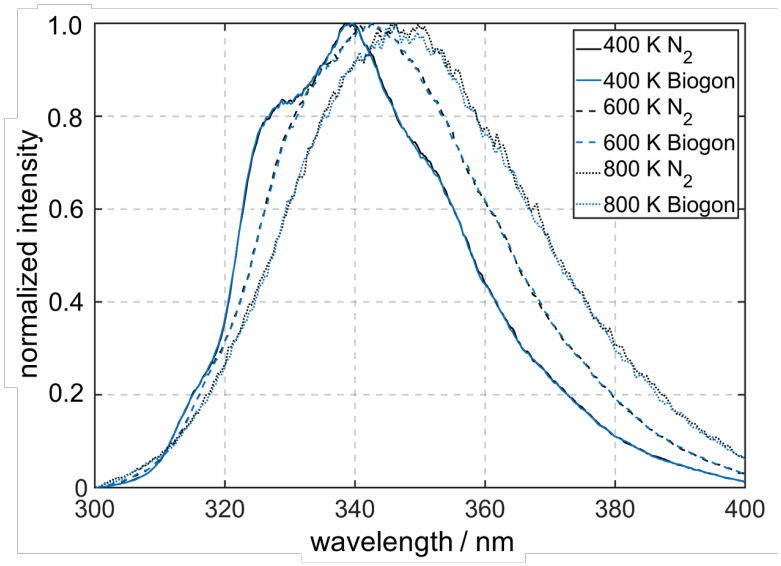

Fig. 1 Temperature dependent fluorescence spectrum of 1-MN in nitrogen or Biogon C20 at 1 MPa (Retzer 2021).

Biogon C20 (Linde) is a mixture of nitrogen and 20% CO_2, which is often utilized for studying effects of exhaust gas components on the fluorescence signal. In principle, the spectra are very similar so that the ambient gas is not expected to affect the LIF signal significantly. However, the LIF signal of 1-MN is different, if e.g. oxygen is included, which is a typical fluorescence quencher, see, e.g. (Retzer et al. 2019).

The temperature dependent signal ratio of two spectral channels (λ_1 and λ_2) is mathematically formulated as follows:

$$S_{\mathrm{ratio}} = \frac{S_{\lambda 1}}{S_{\lambda 2}} = \frac{[\eta_1 \cdot E \cdot n_{\mathrm{tracer}} \cdot \sigma_{\mathrm{abs}}(\lambda_{\mathrm{ex}}, T) \cdot \Phi_{\mathrm{fl}}(\lambda_{\mathrm{ex}}, T, p, \chi_{\mathrm{i}})]_{\lambda 1}}{[\eta_2 \cdot E \cdot n_{\mathrm{tracer}} \cdot \sigma_{\mathrm{abs}}(\lambda_{\mathrm{ex}}, T) \cdot \Phi_{\mathrm{fl}}(\lambda_{\mathrm{ex}}, T, p, \chi_{\mathrm{i}})]_{\lambda 2}} = \frac{[\eta_1 \cdot \Phi_{\mathrm{fl}}(\lambda_{\mathrm{ex}}, T, p, \chi_{\mathrm{i}})]_{\lambda 1}}{[\eta_2 \cdot \Phi_{\mathrm{fl}}(\lambda_{\mathrm{ex}}, T, p, \chi_{\mathrm{i}})]_{\lambda 2}}. \quad (2)$$

The laser fluence E cancels out in the ratio as only one laser is applied for excitation. The same holds true for the number density of the tracer molecules n_{tracer} and the absorption cross section σ_{abs}. The effect of the efficiency of the optical detection system η_i is eliminated by a homogeneous reference image. This reference image (also known as "flat-field correction" or "normalization") is taken at known conditions. This normalization is considered by a division mathematical operation.

For building the signal ratio for 2c-LIF using 1-MN, two long pass filters (LP295 and LP355) are applied. The respective calibration data of planar LIF-measurements generated in a calibration cell in nitrogen atmosphere are provided in Figure 2. Additional calibration functions for further gas mixtures (e.g. different equivalence ratios) can be found elsewhere (Retzer et al. 2019).

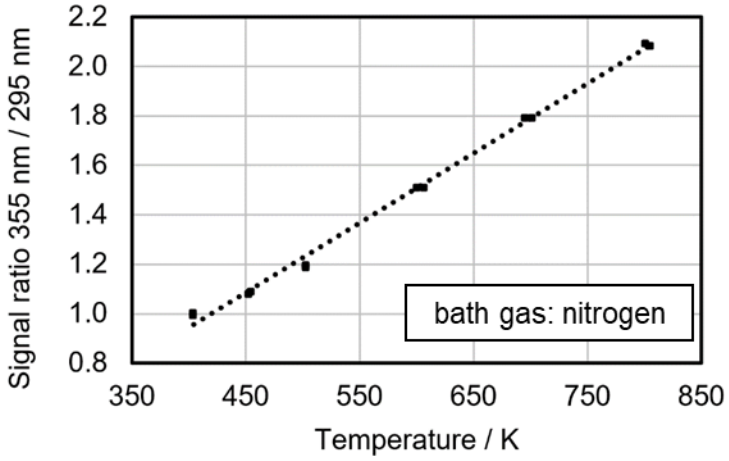

Fig. 2 Calibration function of the temperature dependent fluorescence signal ratio 355 nm / 295 nm in nitrogen including a linear fit function. Data is extracted from (Lind et al. 2017).

3. Experiment

High-speed fluorescence measurements in the RCEM are performed using a high-speed laser (Quasimodo, Spectral Energies), which is operated in a "burst mode" being limited to a time interval of maximum 10 ms. The optical setup at the RCEM is provided in Figure 3.

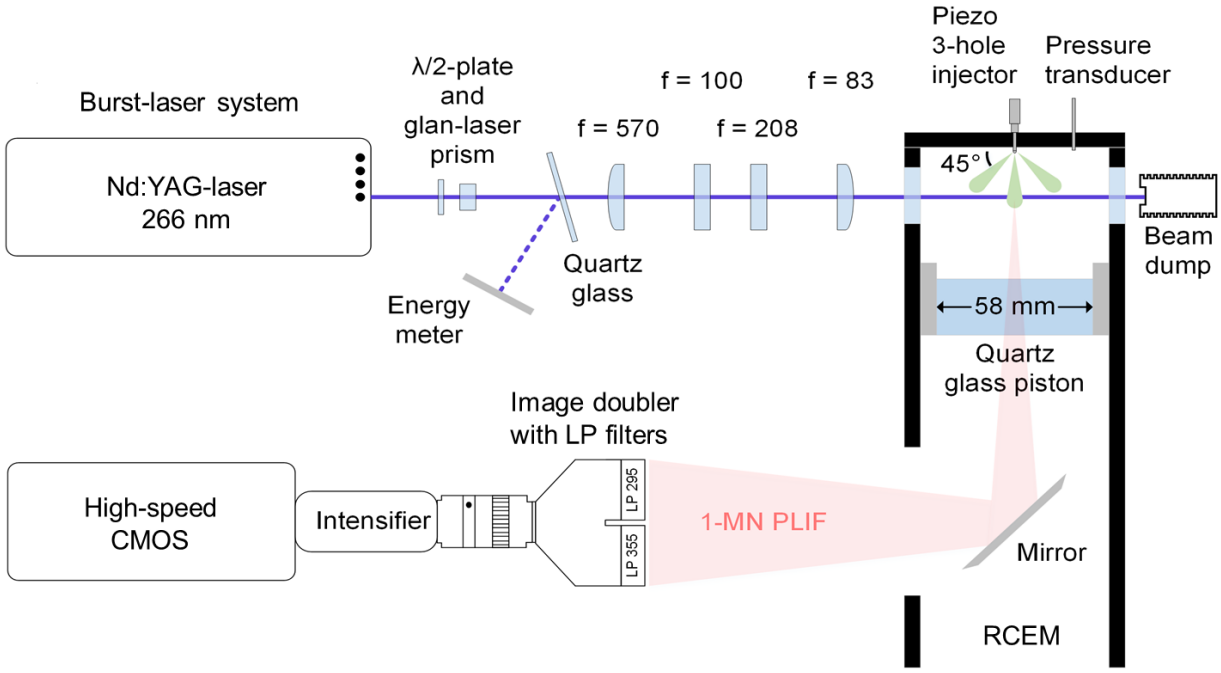

Fig. 3 Optical setup at the RCEM including burst-mode laser, light-sheet forming optics and LIF imaging system

The light sheet formed has a height of about 40 mm and a width of about 0.6 mm. This results in a laser fluence of approximately 15 mJ/cm². The recording frame rate of 7.5 kHz is sufficient for these measurements and reduces damage of optical components by the laser. The fluorescence signal is detected perpendicularly to the light sheet through the quartz glass piston. A high-speed camera is applied in combination with an image doubler (LaVision). This enables the simultaneous recording of two spectral channels for 2c-LIF thermometry (using the LP295 and LP355 filters mentioned above) and measurement of the fuel partial density. The image doubler offers the advantage that only one intensified CMOS camera is necessary.

To minimize possible scattered light from the laser, an additional long pass filter (LP266) is installed in front of each channel. For the determination of the fuel partial density, the channel covering the entire fluorescence spectrum (LP295) is used. All images are corrected with respect to pulse to pulse and burst to burst variation. Furthermore, the laser absorption as a function of

the cylinder volume is considered. Additionally, the temperature dependence of the fluorescence signal must also be corrected, before the fuel partial density is determined.
In the RCEM, the light sheet was positioned in a 3 mm distance from the cylinder head. The resulting region of interest (ROI) within the overlapping region was 11 mm x 10 mm. The ROI comprises 2750 pixels in the center of the light sheet within the cylinder volume. The temperature within a ROI is determined pixel by pixel by normalizing each image to the homogeneous reference image at known temperature and fuel concentration (0.3 MPa, 383 K). The calibration function has to be applied afterwards. The average temperature within this ROI was determined for each individual image and it is utilized for generation of temporal courses during compression. The temperature in the cylinder was determined before the LIF measurements using thermocouples and absorption spectroscopy (Fendt et al. 2021; Retzer et al. 2020). This information is required for measurements of the initial temperature and the reference conditions.

4. Results

In the subsequent sections, the temperature and fuel partial density is measured in the RCEM during compression and expansion. Only experiments in nitrogen atmosphere are presented in the present publication. The fuel (n-heptane, containing 1 vol% tracer) is injected early before start of compression. By this, relatively homogeneous initial conditions are achieved. Temperature and fuel partial density profiles are provided in different compression cycles. A compression process takes about 15 ms to 30 ms from start of compression to top dead center (TDC). This depends on the driving gas pressure. Consequently, the complete compression stroke cannot be covered with just one burst, which covers 10 ms. Thus, for each operating point, three measurements are performed in series, each with a different trigger time (interval 1, 2 and 3), see Figure 4. Each series of measurements is repeated three times (run A, B and C). The experiments are conducted for a driving gas pressure of 4.1 MPa and 0.3 MPa initial cylinder pressure. The temperature rises up to about 770 K (average temperature) at a peak pressure of approximately 6.5 MPa at TDC. The temperature at TDC is about 70 K below the adiabatic compression temperature, which is due to the inhomogeneities of the temperature field close to the cylinder wall at this point in time (see discussion below). After reaching TDC, the temperature is reduced due to the expansion of the gas. The standard deviation of the average temperature is in the range of 1 % for all points in time. Due to the decreasing volume during compression, the determined fuel partial density increases until TDC and decreases again accordingly after TDC. On average, the determined partial density is slightly below the theoretically calculated partial density. The temporal and cyclic variations increase towards TDC. This can be explained by lens effects caused by density gradients in the

measuring volume. These lens effects may lead to a local broadening and thickening of the light sheet, as well as to beam steering and laser sheet inhomogeneities (i.e. line patterns), which may decrease the laser fluence. This could cause a lower or higher local fluorescence intensity, respectively. Furthermore, laser absorption at TDC is very strong due to the high pressure leading to a reduced SNR. In general, the SNR is much lower close to TDC (at temperatures of about 800 K). It may drop about 65% (from 500 K to 800 K) to ~10 for the "red" channel, see also discussion in (Lind et al. 2017). The standard deviation (of single shot images, i.e. shot-to-shot deviations) between the three runs is about 4 % (at 15 ms) and about 6 % at (-5 ms).

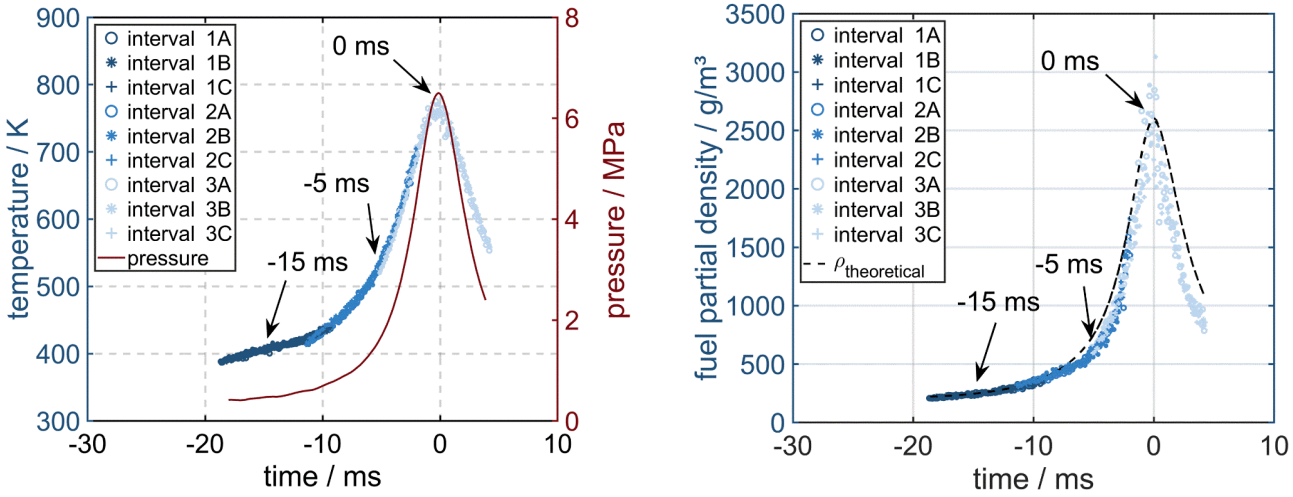

Fig. 4 Temperature (left) and fuel partial density (right) profiles during compression and expansion in the RCEM at 4.1 MPa driving gas pressure; the profile consists of three partially overlapping scans (intervals 1-3); The pressure curve is added (left) as well as the theoretical density profile (right).

Such PLIF measurements are especially useful for studying inhomogeneities in the temperature and fuel partial density dispersion due to the heat transfer at the cool walls. These heat transfer effects become relevant especially close to TDC. They may be much more severe for RCEMs compared to IC engines. Example measurements are presented in the subsequent section.

For deeper insights into spatial temperature and density variations, horizontal plots through the center of the ROI at TDC are provided in Figure 5. Two points in time are compared: -15 ms aTDC (left) and 0 ms (TDC) (right). The corresponding single shot images of the temperature and fuel partial density are provided in the respective diagram. In general, the regions of high fuel partial densities correlate well with low temperatures. The profiles are spatially averaged values calculated from five pixel rows.

At -15 ms, the temperature variation is up to 30 K (average temperature ~405 K, maximum temperature ~428 K, minimum temperature ~387 K) corresponding to density variations between

247 g/m³ and 262 g/m³. As expected, the temperature variations are more distinct at TDC leading to larger differences in fuel partial density as well. Here, cooler gases penetrate from the wall surface into the center of the cylinder as the piston approaches TDC. Furthermore, the typical large scale roll-up vortices that occur in RCMs/RCEMs may intensify these inhomogeneities (Goldsborough et al. 2017). The dimensions of occurring cool regions are in the range of several millimeters (see the images in the diagram). However, the temperature differences are larger than 300 K (average temperature is about 770 K, maximum temperature ~960 K, minimum temperature ~570 K) at TDC (0 ms, peak pressure of 67 bar) corresponding to density variations between 2500 g/m³ and 3700 g/m³. Even in other RCMs/RCEMs, no such large temperature variations were observed. They were typically below 200 K in the near-wall region, see e.g. (Goldsborough et al. 2017). However, the pressure and temperature level may not be fully comparable due to different designs of the RCM/RCEM or different geometries of the combustion chamber. In principle, such temperature distributions appear also in piston engines at TDC due to heat transfer effects at the cylinder head (Dec and Hwang 2009). However, the temperature drop is much larger in the present RCEM than in IC engines due to its cooler cylinder walls, as there is no continuous operation.

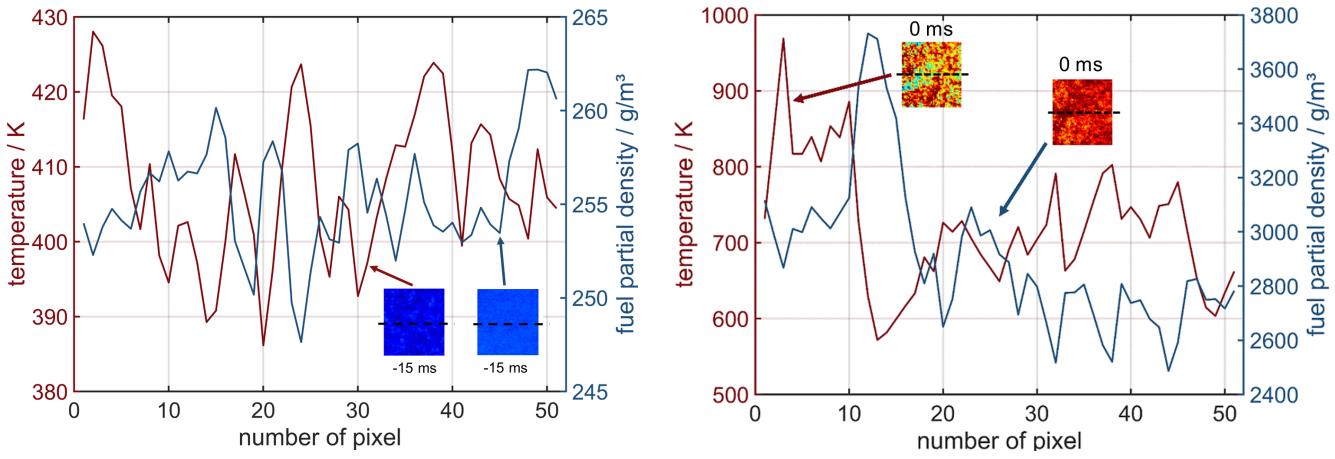

Fig. 5 Horizontal plots of temperature and fuel partial density profiles in the center of the ROI at -15 ms aTDC (left) and at TDC (0 ms, right).

Typically, there is only one compression measurement possible within approximately 3 min for the present RCEM, so that the inner wall temperature is probably much lower compared to IC engines. For example, Dec and Hwang (Dec and Hwang 2009) observed temperature variations of about ±50 K at TDC in a motored Diesel IC engine in a measurement plane 4 mm below the firedeck. The

average temperature was about 1000 K at 40 bar, which was estimated by using an adiabatic model and 1c-PLIF.

These observed larger temperature inhomogeneities at TDC in the RCEM lead to deviations from adiabatic conditions, which are usually assumed in compression models. These inhomogeneities may affect the calibration inside the cylinder itself as well as ignition, combustion and pollutant formation in the RCEM. Consequently, they need special consideration and a quantitative planar measurement technique for resolving such gradients. For this purpose, a high-speed 2c-LIF technique as proposed in this contribution is thus advantageous.

5. Conclusions and outlook

Two-colour planar laser-induced fluorescence of 1-MN was utilized for determination of temperature and fuel partial density courses during compression in a RCEM. A recording frame rate of 7.5 kHz was applied. Measurements were conducted under homogeneous mixing conditions in nitrogen atmosphere. The calibration data generated in a flow cell was used as the basis for thermometry and for determination of fuel partial density. Average temperatures up to 820 K were detected while local maximum temperatures exceeded 900 K. Inhomogeneities were observed in terms of partially large structures and gradients in the temperature and fuel partial density fields. They occurred near the cylinder wall during compression, especially at TDC. These inhomogeneities are due to the heat transfer between the hot gas and the cool walls. The measured spatial temperature differences are larger than 300 K. These large differences have not been observed in other measurements in IC engines or RCMs. This may be attributed to the special design of the RCEM.

In future, measurements using LIF under very challenging transcritical and supercritical conditions will be performed. These conditions are present in diesel IC engines and rocket combustors but also in many other processes in chemical engineering or pharmaceutical applications. For this purpose, the PLIF technique must be optimized and complemented for detection of liquid and vapor zones, and for the transition to supercritical conditions. Consequently, special calibration setups and measurements are required, which are currently under preparation.

Acknowledgements

The authors acknowledge funding by Deutsche Forschungsgemeinschaft (DFG Zi 1384/3).

We would like to thank Andreas Peter as well as Peter Fendt at LTT Erlangen for supporting the measurements. The authors gratefully acknowledge funding of the SAOT by the Bavarian State Ministry for Science and Art.

References

Dec, J. E., Hwang, W. (2009). Characterizing the development of thermal stratification in an HCCI Engine using planar-imaging thermometry. *SAE International Journal of Engines* 2, 421-438

Fendt, P., Brandl, M., Peter, A., Zigan, L., Will, S. (2021). Herriott cell enhanced SMF-coupled multi-scalar combustion diagnostics in a rapid compression expansion machine by supercontinuum laser absorption spectroscopy. *Optics Express* 29, 42184-42207

Goldsborough, S. S., Hochgreb, S., Vanhove, G., Wooldridge, M. S., Curran, H. J., Sung, C.-J. (2017) Advances in rapid compression machine studies of low- and intermediate-temperature autoignition phenomena. *Progress in Energy and Combustion Science* 63, 1-78

Lind, S., Retzer, U., Will, S., Zigan, L. (2017). Investigation of mixture formation in a diesel spray by tracer-based laser-induced fluorescence using 1-methylnaphthalene. *Proceedings of the Combustion Institute* 36, 4497-4504.

Peterson, B., Baum, E., Böhm, B., Sick, V., Dreizler, A. (2015). Spray-induced temperature stratification dynamics in a gasoline direct-injection engine. *Proceedings of the Combustion Institute* 35(3), 2923-2931.

Peterson, B., Baum, E., Böhm, B., Sick, V., Dreizler, A. (2014). Evaluation of toluene LIF thermometry detection strategies applied in an internal combustion engine. *Applied Physics B* 117, 151-175

Retzer, U., Fink, W., Will, T., Will, S., Zigan, L. (2019). Fluorescence characteristics of the fuel tracer 1-methylnaphthalene for the investigation of equivalence ratio and temperature in an oxygen-containing environment. *Applied Physics B* 125, 124

Retzer, U., Ulrich, H., Bauer, F.J., Will, S., Zigan, L. (2020). UV absorption cross sections of vaporized 1-methylnaphthalene at elevated temperatures. *Applied Physics B* 126, 50

Retzer, U. (2021). *Gemischbildungsanalyse mit der laserinduzierten Fluoreszenz: Von der Tracercharakterisierung zur Hochgeschwindigkeitsanwendung*. Dissertation, FAU Erlangen-Nürnberg, Erlangen, 2021

Schulz, C., Sick, V. (2005). Tracer-LIF diagnostics: quantitative measurement of fuel concentration, temperature and fuel/air ratio in practical combustion systems. *Progress in Energy and Combustion Science*, 31(1), 75-121.

Tran, K. H., Morin, C., Kühni, M., Guibert, P. (2014) Fluorescence spectroscopy of anisole at elevated temperatures and pressures. *Applied Physics B* 115, 461–470.